Journal of the Brazilian Society of Mechanical Sciences and Engineering (2020) 42:486
https://doi.org/10.1007/s40430-020-02540-x

TECHNICAL PAPER

Design sensitivity and optimization of powertrain mount system design parameters for rigid body modes and kinetic energy distributions

Polat Şendur[1] · **Birkan Tunç**[2]

Received: 19 August 2019 / Accepted: 30 July 2020 / Published online: 24 August 2020

Abstract

This study evaluates the influences of the powertrain mount design parameters on the frequencies of powertrain rigid body modes and their kinetic energy distributions (KEDs), which play an important role in the low-frequency vibration of vehicles. A total of 12 design parameters (x, y, z position of mount locations and translational stiffness of the front and rear powertrain mounts) were evaluated in terms of their contributions to the aforementioned metrics. A multi-body dynamics simulation model was used in a 512-run modal analysis by varying the design variables across their common range, and the results were used in design sensitivity analysis. Response surface models for the frequencies of each powertrain rigid body mode and their KEDs were derived and subsequently used in optimization studies. It was shown that front and rear powertrain mount stiffness in y-direction has a strong influence on the frequency of powertrain lateral mode (21.5% and 24.5%, respectively). Front mount location in the x-direction demonstrates a strong influence on the pitch mode (25.7%), while the rear mount stiffness in the z-direction is the most influential on frequency of powertrain vertical mode with 29.1%. The location of the rear powertrain mount in the z-direction has a significant effect on the KED of fore-aft mode with 37.8% sensitivity. NSGA-II genetic algorithm with 100 generations was used for optimization to meet a set of design targets compiled from the literature. For the placement of the frequencies of powertrain rigid body modes with desired KED, design sensitivities, which are derived from a system-level approach, give important design direction to address the complex interactions between powertrain mount locations and stiffness and key metrics of the powertrain mount systems. Knowledge of design sensitivity of design parameters is important in the vehicle design cycle for OEMs to prioritize their design decisions. Finally, the optimization methodology is key to tune the design parameters to meet the conflicting design targets more efficiently.

Keywords Modal analysis · Powertrain rigid body modes · Powertrain mount design · Design sensitivity · Optimization

Abbreviations

x_g	Longitudinal position of the powertrain center of gravity
y_g	Lateral position of the powertrain center of gravity
z_g	Vertical position of the powertrain center of gravity
m	Mass of powertrain system
I_{xx}	Mass moment of inertia of powertrain with respect to x-axis of powertrain inertia coordinate system
I_{yy}	Mass moment of inertia of powertrain with respect to y-axis of powertrain inertia coordinate system
I_{zz}	Mass moment of inertia of powertrain with respect to z-axis of powertrain inertia coordinate system
I_{xy}	Product of inertia of powertrain with respect to x–y-axis of powertrain inertia coordinate system
I_{xz}	Product of inertia of powertrain with respect to x–z-axis of powertrain inertia coordinate system

Technical Editor: Wallace Moreira Bessa.

✉ Polat Şendur
polat.sendur@ozyegin.edu.tr

Birkan Tunç
birkan.tunc@yeditepe.edu.tr

[1] Ozyegin University, 34794 Cekmekoy, Istanbul, Turkey

[2] Yeditepe University, 34755 Atasehir, Istanbul, Turkey

I_{yz}	Product of inertia of powertrain with respect to y–z-axis of powertrain inertia coordinate system
x_{fr}	Front powertrain mount longitudinal position
y_{fr}	Front powertrain mount lateral position
z_{fr}	Front powertrain mount vertical position
x_{rr}	Rear powertrain mount longitudinal position
y_{rr}	Rear powertrain mount lateral position
z_{rr}	Rear powertrain mount vertical position
K_{fx}	Front powertrain mount longitudinal stiffness
K_{fy}	Front powertrain mount lateral stiffness
K_{fz}	Front powertrain mount vertical stiffness
K_{rx}	Rear powertrain mount longitudinal stiffness
K_{ry}	Rear powertrain mount lateral stiffness
K_{rz}	Rear powertrain mount vertical stiffness
KED	Kinetic energy distribution
KED(n,i)	KED of the ith mode in the nth DOF
LHS	Latin hybercube sampling
RSM	Response surface model
PRCC	Partial ranked correlation coefficients
$PRCC_{k,i}$	PRCC of the ith input on the kth output
% $Sensitivity_{k,i}$	Sensitivity of the ith input on the kth output
f_{fa}	Frequency of powertrain fore-aft mode
f_{l}	Frequency of powertrain lateral mode
f_{v}	Frequency of powertrain vertical mode
f_{r}	Frequency of powertrain roll mode
f_{p}	Frequency of powertrain pitch mode
f_{y}	Frequency of powertrain yaw mode
KED_{fa}	KEDs for powetrain fore-aft mode
KED_{l}	KEDs for powertrain lateral mode
KED_{v}	KEDs for powertrain vertical mode
KED_{r}	KEDs for powertrain roll mode
KED_{p}	KEDs for powertrain pitch mode
KED_{y}	KEDs for powertrain yaw mode
NSGA-II	Nondominated sorting genetic algorithm

1 Introduction

Noise and vibration are among the top factors related to quality in vehicle design [1]. They are considered as the key components for the isolation of powertrain forces in addition to its primary function of supporting the weight of the powertrain. Although they may be considered as simple structures, there is an extensive literature review on powertrain mount systems, functions and challenges related to their design [2, 3].

Powertrain mounting systems have various types including elastomeric, hydraulic, passive and active mounts. Passive rubber mounts are simple rubber elements providing stiffness and damping [4–6]. Jung et al. [7] demonstrated the ability of such mounts for vibration isolation over a wide frequency range. The hydraulic mounts are advantageous in terms of the trade-offs between the static and dynamic design targets [8]. There is an extensive literature on the analysis and optimization of such mounts [9–11]. With recent advances, active powertrain mount applications were frequently used in order to control the powertrain-induced vibrations [12]. The cost, maintenance, and reliability of powertrain mounts have been addressed [5].

There are many challenges related to powertrain mount systems due to the trade-offs between various design targets and their complex relation to design parameters. The stiffness of a typical elastomeric mount increases with increasing frequency, which results in poor vibration isolation at higher frequencies. However, low stiffness values are not desired since they may lead to large static displacement [8]. Advances in simulation technology have become a key enabler to address the aforementioned trade-offs in the design. A wide variety of simulation tools ranging from finite element models and multi-body dynamics [1] have become industry standard due to their high accuracy on the predictions.

The development of the powertrain mount systems in the automotive product development cycle focuses on the structural optimization of the powertrain mounts and optimization of the mount stiffness and positions. The former is generally performed using finite element-based models using topology optimization methods, while the latter mostly deals with the rigid body-based models using design optimization methods.

There are many studies in the literature on the structural optimization of the powertrain mount structures. For example, results from three commercial software programs on topology optimization are compared to each other for the powertrain mount design in terms of their computational efficiency and optimum solution [13]. Similarly, the application of a multi-objective optimization algorithm to optimize the dimensions of a powertrain mount design is demonstrated using a finite element model of the powertrain mount. The weight, first mode of the powertrain mount, and the maximum von Mises stress are the objective functions [14]. In another study, a topology optimization algorithm is applied to an elastomeric powertrain mount to achieve desired stiffness characteristics in two directions using a finite element based model of the rubber block and experimental data [15]. The application of a topology optimization algorithm is presented to minimize the weight for a powertrain mount of an aircraft under the loads on an airplane according to the code of Federal Regulations [16]. A significant reduction in the volume ratio of the structure is achieved according

to structural stress and buckling constraints in this study. In a very recent study, structural optimization of a powertrain mount has been performed by integrating static, modal, and frequency response analyses. The comparisons between the original and the optimized designs were made on the natural frequencies of the structure, von Mises stress, and amplitude of the frequency response. Besides, the weight and cost of material and manufacturing are considered as important design factors [17].

There are many studies in the literature for the minimization of the vibration transmissibility of the powertrain mount by integrating the rigid body models and the design optimization tools. For example, various optimization techniques such as sequential quadratic programming for the mount locations and orientations are employed to minimize the vertical force transmitted [18, 19]. In the studies, which are based on the optimal placement of the frequencies of rigid body modes, powertrain modes are decoupled from each other where the location and orientation of the powertrain mounts are chosen as design parameters [20–22]. Swanson et al. [23] compared the base and the optimum designs obtained from the minimization of the transmitted forces and the placement of the frequencies of powertrain rigid body modes. Ashrafiuon [24] optimized the aircraft powertrain mount system using the closed form of the derivatives of amplitudes of vibrations. In another study, Christopherson and Jazar [25] optimized a hydraulic mount to minimize various frequency response functions. The theory of energy decoupling is used by Yonghou and Guocai [26] to optimize the powertrain mount system by choosing the objective function as the maximization of the decoupling rate. Finally, torque roll axis decoupling and optimization methods were considered in various studies [27–30] to determine the best position of powertrain mounts for various operating conditions. Liette et al. [31] proved that the decoupling of the torque roll axis is not viable for powertrain applications and examined alternative isolation systems. The application of multi-objective and evolutionary optimization algorithms has been used more recently on the optimization of powertrain mount systems. For example, the stiffnesses of the powertrain mounts in three directions are optimized by the application of a combined genetic algorithm and robustness analysis. The optimization performance is quantified by comparing time and frequency domain results of the optimized and original design under powertrain and road excitations [32]. In more recent studies, coupling effects of different subsystems including the powertrain mount systems were taken into account to provide vibration isolation between the subsystems using a 15 DOF full vehicle model [33]. A multi-objective optimization algorithm is proposed as an integration of genetic algorithm, neural networks, and evolutionary algorithms using a 10 DOF full vehicle model. Six objective functions include the mean square displacement and the acceleration of powertrain mounts, where the stiffnesses of each mount are the design variables [34]. The time and frequency domain comparisons on three different powertrain mount materials were made experimentally in terms of the vibration isolation characteristics and their life [35]. The study suggests that a combination of materials provides improved vibration performance than natural rubber. In a more recent study, the powertrain mounting system of an electric vehicle is optimized where the performance of the application of particle swarm optimization is improved by coupling it with NSGA-III algorithm [36]. The multi-objectives include the mean square acceleration and mean square displacement of the powertrain mount system. In [37], the authors integrated the rigid body models and structural optimization of the powertrain mount structure using topology optimization. For the former, the objective functions are the frequencies of the powertrain modes and their coupling, where the hardness of each mount is optimized. For the latter, the topology of the structure is determined by the application of the topology optimization, where an objective function considers the static and dynamic characteristics of the structure. In the topology optimization, the critical location is determined from a previous analysis of the structure under the operational loads from the transmission and road [37].

Besides the simulation and optimization of the powertrain mount system, there are studies related to the uncertainties of powertrain mount system design in the literature. For example, the fatigue life of powertrain mount systems is determined using Monte Carlo taking into account the variability of important parameters based on experience [38]. A new method is proposed by considering the hybrid uncertainties between the natural frequency and decoupling ratios of the powertrain mounting systems thereby taking into account the uncertainties associated with the powertrain mount system [39]. In a recent study, a MOGA optimization algorithm is applied to a powertrain mount system by taking into account the variability of the design variables from experimental data [40]. In this study, system-level design variables such as spring stiffness and subsystem-level system variables such as rubber dimensions are optimized where the constraints are related to the frequencies and their separation, and upper limit on strain values.

Though it is not as common as optimization of the passive mounts, active control of powertrain mounts has been the subject of research in recent years. For example, Bian et al. developed control algorithms for modifying the frequency and damping [41]. They demonstrated the methods theoretically and experimentally to reduce the nonlinear torsional vibration of the powertrain system. In another study, active control of powertrain mounts of hybrid electric vehicles (HEVs) was proposed for the improvement of vibration isolation during engine-start and engine-stop operations [42].

Concurrently NVH, durability, vehicle dynamics, safety, performance, and cost expectations have become more and more stringent, necessitating robust and efficient system modeling and design optimization/control procedures. Therefore, the need for formal design methodologies, which can explore the synergistic effects of coupling between design parameters at every phase of the design process, is increasing. In the past, mathematical models for structural and rigid body dynamics have been developed for the isolation of powertrain excitation, and various optimization algorithms have been exploited for a better understanding of powertrain mount systems. However, to the author's best knowledge, no studies have quantified the sensitivity of primary powertrain mount design parameters across all the major NVH key performance indices and design targets. Moreover, the optimization of the full set of design targets using rigorous and versatile engineering methods is limited. Such an approach would be beneficial for automotive OEMs from many aspects: (1) They will be able to address the uncertainties in their powertrain mount system design. More specifically, uncertainties on material properties such as Young's modulus and endurance limit and variations in the stiffness of mount parameters may result in the variation in the frequencies of powertrain modes and their coupling. The indeterministic nature of the parameters may adversely affect system performance and customer perception in terms of vehicle dynamics and NVH. Instead, the concept of safety factors is generally introduced to account for uncertainties in the material properties and other design parameters. However, since the selection of factor of safety is mostly based on the experience of the automotive OEMs, there is always a risk of not meeting functional targets or designing over-engineered systems. Therefore, knowing the sensitivities of design parameters on key performance metrics is of great importance, and (2) determination of the frequencies of system/subsystem modes and their modes is a common task in the automotive industry. This information is used to distribute the frequencies of the system so that they are separated from each other and/or from excitation frequencies. This process, which is known as modal alignment, is highly dependent on the sensitivities of the mode frequencies. So if the modal alignment is not robust, system modes and excitations may couple at one or more frequencies resulting in poor NVH performance. The information on the sensitivity of design parameters on powertrain rigid body modes and their coupling will increase the robustness on the modal alignment. The originality of this work stems primarily from the integration of sensitivity of design parameters on design targets to understand the coupling of these subsystems and their effect on powertrain mount systems. The knowledge of the sensitivity of design parameters on key metrics fills the gap of taking into account the robustness of the system. Therefore, this paper presents a complete design process of the powertrain mounting system, including the vibration decoupling, vibration simulation analysis, and multi-objective optimization. The objective of the current study is to better understand the sensitivity of primary design factors across all powertrain rigid body modes and their kinetic energy distributions.

The organization of the paper is as follows: first, methodology including the modeling, design sensitivity, and optimization with the full set of design targets compiled from literature are described in Sect. 2. Then, the results of variational study, sensitivity analysis, and design optimization are discussed in Sect. 3. Finally, the last section is reserved for the conclusions and future work.

2 Materials and methods

2.1 Description of the mathematical model

The mathematical modeling employs a representation of a vehicle powertrain with four bushings represented by three translational springs in longitudinal, lateral, and vertical directions. The model has only one rigid body representing the powertrain system. The rigid body has 6 degrees of freedom as it is free to translate and rotate in all directions. The powertrain system is connected to ground by 4 bushings, which represent the powertrain mounting system. This type of modeling represents the powertrain mounts between the chassis and the powertrain system. This modeling approach is commonly used in the literature [37, 39, 43]. The global coordinate system at the center of mass of the powertrain at the static equilibrium is shown in Fig. 1,

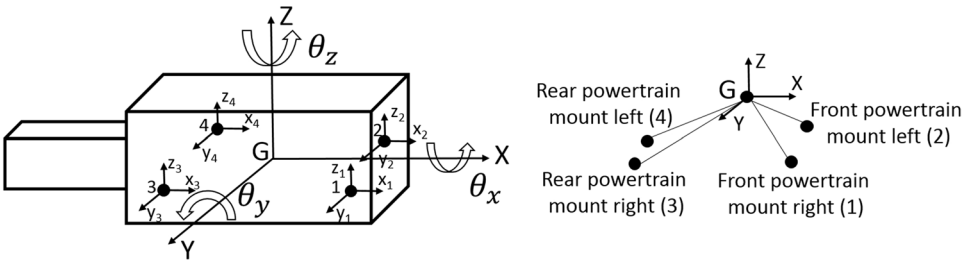

Fig. 1 Sketch of the powertrain mount system model

while the corresponding ADAMS model with six degrees of freedom (DOF), is presented in Fig. 2.

The parameters of the powertrain mount system are given in Table 1.

2.2 Rigid body modes and their KEDs

The frequencies of the powertrain rigid body modes are calculated by solving the eigenvalue problem as described by [44]. A static analysis is performed first to find the static equilibrium of the system using the ADAMS model. Then, the normal mode analysis is performed about this static equilibrium position to determine the frequencies of the powertrain rigid body modes using built-in ADAMS/Vibration toolbox. Kinetic energy distribution (KED) is another performance metric as a measure of decoupling between modes. %100 decoupling, which is desirable for vibration performance, is only possible at certain configurations [45]. KED is defined as the ratio of the kinetic energy of a mode to the overall energy of all the modes corresponding to a specific frequency. As the powertrain vibrates at a natural frequency, w_i (n = 1,2,3,4,5,6), the kinetic energy distribution of the mode as percentage in the n DOF (n = 1,2,3,4,5,6) of the powertrain and ith order mode, KED(n, i) is calculated according to Eq. (1) [39]:

$$\mathrm{KED}(n,i) = \frac{\phi_{ni} \cdot \sum_{l=1}^{6} M_{nl} \cdot \phi_{li}}{\phi_i^T \cdot M \cdot \phi_i} \cdot 100 \tag{1}$$

where M is the 6×6 mass matrix of the powertrain system, ϕ_{ni} is the element of mode shape matrix, ϕ (6×6 matrix), corresponding to the n^{th} row and i^{th} column, ϕ_{li} s the element of ϕ, corresponding to l^{th} row and i^{th} column, and ϕ_i is the mode shape vector corresponding to i^{th} natural frequency, i.e., $\phi_i = \{\phi_{1i}, \phi_{2i}, \phi_{3i}, \phi_{4i}, \phi_{5i}, \phi_{6i}\}$. M_{nl} is the element of the mass matrix, M, corresponding to the n^{th} row and l^{th} column.

Table 1 The parameters of the MSC.ADAMS model

x_g, y_g, z_g (mm)	(3450, 5, 1200)
Powertrain mass, m (kg)	1550
(I_{xx}, I_{xy}, I_{yy}, I_{xz}, I_{yz}, I_{zz}) (kg m^2)	(138, −2.35, 843, 135, 0.53, 768)
Front-left powertrain mount position (x, y, z) (mm)	(2600, −400, 1250)
Front-right powertrain mount position (x, y, z) (mm)	(2600, 400, 1250)
Rear-left powertrain mount position (x, y, zz) (mm)	(3800, −400, 1150)
Rear-right powertrain mount position (x, y, z) (mm)	(3800, 400, 1150)
Front powertrain mount stiffness (x, y, z) (N/mm)	(800, 300, 1200)
Rear powertrain mount stiffness (x, y, z) (N/mm)	(9000, 2500, 3500)

For more detailed description and derivation of the KED, the reader is referred to [39]. The kinetic energy distribution of each mode for each frequency is obtained from the ADAMS/Vibration toolbox according to Eq. (1).

2.3 Variational design study

A Design of Experiment (DoE) set containing 512 runs was obtained by Sobol sequence varying key design factors. Powertrain mount stiffness was varied by ±20% [4]. Front and rear powertrain mount locations are varied with a similar approach as in [18, 22]. Nominal values and variation of design factors are shown in Table 2, where x_{fr}, y_{fr}, z_{fr} are the longitudinal, lateral, and vertical locations of front powertrain mounts, x_{rr}, y_{rr}, $z_{\mathrm{rr}}$are the longitudinal, lateral, and vertical locations of rear powertrain mounts, K_{fx}, K_{fy}, K_{fz}, K_{rx}, K_{ry}, $K_{\mathrm{rz}}$are front longitudinal, front lateral,

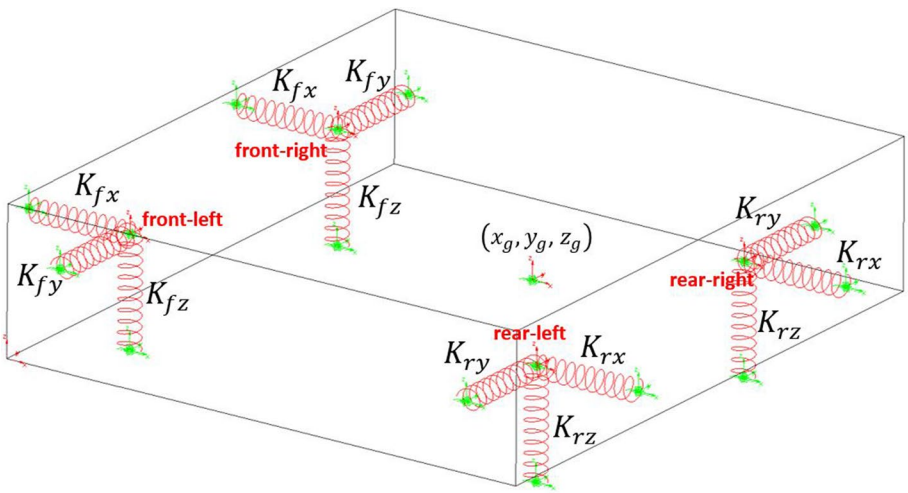

Fig. 2 ADAMS model of the powertrain mounting system

Table 2 Variation on design variables

Design variable	Nominal	Variation (±)
x_{fr} (mm)	2600	100
y_{fr} (mm)	400	50
z_{fr} (mm)	1250	100
x_{rr} (mm)	3800	100
y_{rr} (mm)	400	50
z_{rr} (mm)	1150	100
K_{fx} (N/mm)	800	160
K_{fy} (N/mm)	300	60
K_{fz} (N/mm)	1200	240
K_{rx} (N/mm)	9000	1800
K_{ry} (N/mm)	2500	500
K_{rz} (N/mm)	3500	700

front vertical, rear longitudinal, rear lateral, rear vertical stiffness values, respectively.

Sobol sequence was chosen as the sampling algorithm of the design variables due to its ability to generate more uniformly distributed design space compared to other methods such as Latin Hypercube sampling (LHS). The algorithm to obtain the Sobol sequence is explained in [46] in great detail. The rear powertrain mount stiffness in z-direction based on Sobol and LHS are shown in Figs. 3 and 4, respectively.

2.4 Response surface methodology

The objective of the response surface models is to develop empirical equations relating the design parameters to powertrain rigid body models and their KEDs. These equations would then help the designer determine the design parameters to change the modes and their KEDs by the desired amount by simply using the empirical formulas.

The response surface models (RSM) for the frequencies of the rigid body modes and their KEDs are generated using MATLAB's "lsqcurvefit" function. The DoE set containing 512 samples from the SOBOL sequence was used to construct RSMs. A linear relationship between output and inputs in the

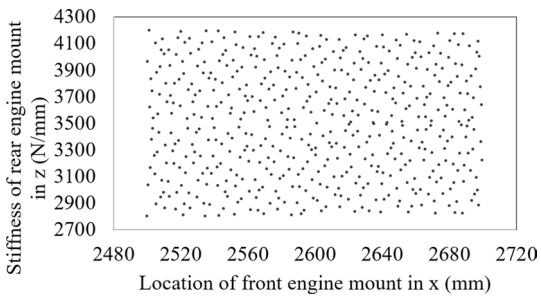

Fig. 3 Sobol sampling algorithm

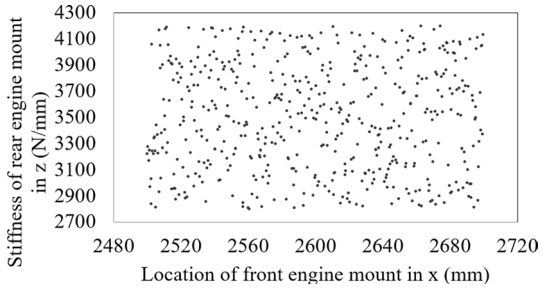

Fig. 4 Latin hypercube sampling (LHS) algorithm

form shown in Eq. (2) is given for the frequency of powertrain vertical mode.

$$f_v = c_0 + c_1 \cdot x_{fr} + c_2 \cdot y_{fr} + c_3 \cdot z_{fr} + c_4 \cdot x_{rr} + c_5 \cdot y_{rr} + c_6 \cdot z_{rr} + c_7 \cdot K_{fx} + c_8 \cdot K_{fy} + c_9 \cdot K_{fz} + c_{10} \cdot K_{rx} + c_{11} \cdot K_{ry} + c_{12} \cdot K_{rz} \quad (2)$$

where f_v is the frequency of powertrain vertical mode, c_0 to c_{12} are the coefficients of the RSM model. Similar expressions were derived for frequencies of powertrain fore-aft (f_{fa}), lateral (f_l), roll (f_r), pitch(f_p) and yaw modes (f_y) as well as their KEDs. RSM models were used in the design optimization study as described in Sect. 2.6.

2.5 Design sensitivity

The sensitivity of design parameters on key metrics of the powertrain mount system is important to determine the modal characteristics of the rigid body modes. Once the most influencing factors are determined, one can modify the values of the parameters to obtain the desired performance.

Since the interaction of the model parameters is unknown and the large variation of the parameters may lead to nonlinear relations between input and output parameters, partial ranked correlation coefficients (PRCC) were used to measure correlation between them [47–50]. PRCC is a robust sensitivity analysis method, which provides a measure of the monotonicity of input and output variables. The correlation coefficients between input variable $\mathbf{x}_j$ and output variable $\mathbf{y}_k$ are calculated as given in Eq. (3):

$$r_{\mathbf{x}_j\mathbf{y}_k} = \frac{\sum_{i=1}^{N} (x_{ij} - \bar{x}_j).(y_{ik} - \bar{y}_k)}{\sqrt{\sum_{i=1}^{N} (x_{ij} - \bar{x}_j)^2 . \sum_{i=1}^{N} (y_{ik} - \bar{y}_k)^2}} \quad (3)$$

where x_{ij} and y_{ik} are sampled data of input and output variables, i represents the sample number where N is the sample size, $\bar{x}_j$ and $\bar{y}_k$ are the respective mean of the sample. If $\mathbf{x}_j$ and $\mathbf{y}_k$ are raw data, $r_{\mathbf{x}_j\mathbf{y}_k}$ is called Pearson correlation coefficient, and if they are rank transformed data, $\mathbf{X}_j$ and $\mathbf{Y}_k$, are used it is called rank or Spearman correlation coefficient

[50]. PRCC between $\mathbf{x}_j$ and output variable $\mathbf{y}_k$ is the correlation coefficient, excluding the effect of remaining variables, calculated using two residuals: $(\mathbf{X}_j - \hat{X}_j)$ and $(\mathbf{Y} - \hat{Y}_k)$ in Eq. (3), and is given in Eq. (4).

$$PRCC_{\mathbf{x}_j\mathbf{y}_k} = \frac{\sum_{i=1}^{N}(X_{ij} - \hat{X}_j)\cdot(Y_{ik} - \hat{Y}_k)}{\sqrt{\sum_{i=1}^{N}(X_{ij} - \hat{X}_j)^2 \cdot \sum_{i=1}^{N}(Y_{ik} - \hat{Y}_k)^2}} \tag{4}$$

where $\hat{X}_j$ and $\hat{Y}_k$ and given in Eq. (5) and Eq. (6).

$$\hat{X}_j = c_0 + \sum_{\substack{p=1 \\ p\neq j}}^{n} c_p \cdot X_p \tag{5}$$

$$\hat{Y}_k = b_0 + \sum_{\substack{p=1 \\ p\neq j}}^{n} b_p \cdot X_p \tag{6}$$

where $c_{0\ldots n}$ and $b_{0\ldots n}$, are the coefficients obtained by linear regression and n is the total number of input variables. $\hat{X}_j$ and $\hat{Y}_k$ are evaluated at each increment i in Eq. (4).

PRCCs were obtained between 12 design variables and 6 frequencies for powertrain rigid body modes and their KEDs. The sensitivity of the input variables on the output variables is generally represented as percentage sensitivity by normalizing each PRCC coefficient for an output variable by the sum of absolute values of PRCCs of input variables corresponding to that output variable as given in Eq. (7).

$$\%Sensitivity_{k,j} = \frac{\left|PRCC_{k,j}\right|}{\sum_{i=1}^{12}\left|PRCC_{k,j}\right|}.100 \quad (j,k = 1,\ldots,12) \tag{7}$$

where k is the output variable (such as yaw mode), j is the input variable (such as the location of front powertrain mount) and $\%Sensitivity_{k,j}$ is the sensitivity of the j^{th} input on the k^{th} output.

2.6 Design optimization

The primary function of powertrain mount system is to provide isolation from powertrain-related excitations as a part of vehicle noise, vibration, and harshness (NVH) targets. This is a quite complex and challenging task in automotive product development cycle considering the package space limitations and powertrain power performance. Therefore, the powertrain mount design must continue to improve while satisfying important design targets on NVH, performance, and low cost. Hence optimization is a proven formal method for designing complex systems with rigor. This section follows a traditional task of meeting conflicting design targets compiled from the literature [21, 39, 45, 51].

The aforementioned sensitivity methodology is helpful to make modifications to the powertrain mount design as it quantifies the contribution of each design parameter on the frequencies of powertrain rigid body mode and kinetic energy distribution associated with that mode. However, the application of formal optimization methods to the powertrain mount design can result in a more cost-effective and feasible design. Besides, the determination of the parameters would be more systematic. For that purpose, the following optimization problem is formulated using the aforementioned design targets from the literature:

- **Design Target 1**: Separation of main combustion excitation frequency with the frequency of powertrain roll mode frequency is essential for good vibration isolation. This requires that the ratio of excitation frequency at idle speed to the roll mode is at least $\sqrt{2}$ [45]. Therefore, the target frequency of powertrain roll mode has been set to 18 Hz with KED of 90%.
- **Design Target 2**: The frequency of the powetrain vertical mode should be between 8 Hz and 10 Hz with at least 90% KED for adequate separation from suspension hop mode [21].
- **Design Target 3**: The frequencies of powertrain rigid body modes should be separated by at least 10% for improved NVH performance [51].
- **Design Target 4**: The frequencies of powertrain fore-aft, lateral, pitch, and yaw modes should have at least 80% KED in their primary direction [21].
- **Design Target 5**: The lowest frequency of powertrain rigid body mode should be greater than 7 Hz to be outside of the human sensitivity and the highest frequency of powertrain rigid body mode should be lower than 20 Hz to be well isolated from vehicle flexible modes [21].

Based on the design targets defined above, design optimization problem is formulated as expressed in Table 3.

Multi-Objective Nondominated Sorting Genetic Algorithm (NSGA-II) was used for optimization due to its efficiency in terms of its constraint handling and higher probability to obtain more uniform pareto optimal solutions [52]. Since the use of RSM models is computationally efficient, 100 generations were used during optimization. This corresponds to 51,200 design alternatives.

Table 3 Formulation of the design optimization problem

Design objectives (Total of 2)

$\text{minimize}[f_r^2 - (18)^2]$

$\text{minimize}[\text{KED}_r^2 - 90^2]$

Design constraints (Total of 24)

$7 < f_p, f_y, f_{fa}, f_l$

$8 < f_v < 10$

$80 < \text{KED}_p, \text{KED}_y, \text{KED}_{fa}, \text{KED}_l$

$1.5 < |f_r - f_l|, |f_r - f_p|, |f_r - f_y|, |f_r - f_{fa}|, |f_r - f_v|, |f_l - f_p|, |f_l - f_y|, |f_l - f_{fa}|, |f_l - f_{fv}|, |f_p - f_y|, |f_p - f_{fa}|, |f_p - f_v|, |f_y - f_{fa}|, |f_y - f_v|, |f_{fa} - f_v|$

Design variables (Total of 12)

$x_{fr}, y_{fr}, z_{fr}, x_{rr}, y_{rr}, z_{rr}, K_{fx}, K_{fy}, K_{fz}, K_{rx}, K_{ry}, K_{rz}$

Variable constraints (Total of 12)

$2500 < x_{fr} < 2700$

$350 < y_{fr} < 450$

$1150 < z_{fr} < 1350$

$3700 < x_{rr} < 3900$

$350 < y_{rr} < 450$

$1050 < z_{rr} < 1250$

$640 < K_{fx} < 960$

$240 < K_{fy} < 360$

$960 < K_{fz} < 1440$

$7200 < K_{rx} < 10{,}800$

$2000 < K_{ry} < 3000$

$2800 < K_{rz} < 4200$

3 Results

This section presents the results for the variational study and the sensitivity results. More specifically, the frequencies of powertrain rigid body modes and their KEDs for the base design configuration are given in Sect. 3.1. Then, the results from the variational design study in Sect. 3.2. The response surface models (RSM) are developed and presented in Sect. 3.3. RSM model can be used in order to calculate the powertrain rigid body modes and their KEDs given a set of design parameters. Besides, these empirical equations will be used in a subsequent optimization study. In Sect. 3.4, we present the sensitivity of design parameters on powertrain rigid body modes and their KEDs. This information is important as it gives which design parameter is effective on the design of powertrain mount system.

3.1 Frequencies of powertrain rigid body modes and their KEDs

Frequencies of powertrain rigid body modes were found to be 8.7 Hz, 8.8 Hz, 11.9 Hz, 12.4 Hz, 17.9 Hz, and 19.2 Hz for lateral, pitch, yaw, vertical, fore-aft, and roll modes, respectively. Modes and corresponding KEDs are shown in Table 4. Fraction of the KEDs for each mode is also shown in Fig. 5. It is shown that the modes with frequencies 8.7 Hz and 11.9 Hz are not pure lateral or yaw modes, instead they are combinations of both, which is not desirable as described in Sect. 2.6.

3.2 Variational design study

Histogram of the frequency of roll mode from Fig. 6 shows that it has the highest variance ranging from 15.6 to 23.0 Hz. The frequency of powertrain yaw mode varies from 8.3 to 14.0 Hz. The minimum variance corresponds to frequency of powertrain vertical mode from 11.1 to 13.8 Hz. The highest variance for the KEDs corresponds to the frequency of powertrain lateral mode from 44.0% to 96.8%, while the lowest variance occurs for the frequency of powertrain pitch mode ranging from 73.7% to 99.9% as shown in Fig. 7. KED for powertrain yaw mode versus yaw

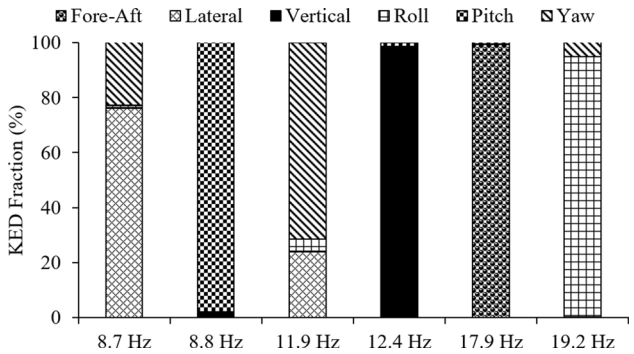

Fig. 5 KED fraction of modes

Table 4 Powertrain modes and corresponding KEDs

Modes (Hz)	Fore-Aft (%)	Lateral (%)	Vertical (%)	Roll (%)	Pitch (%)	Yaw (%)
8.7	0.0	76	0.0	0.8	0.0	23.1
8.8	0.5	0.0	1.4	0.0	98.1	0.0
11.9	0.0	23.9	0.2	4.4	0.0	71.5
12.4	0.0	0.0	98.4	0.0	1.4	0.2
17.9	99.3	0.0	0.0	0.2	0.6	0.0
19.2	0.1	0.1	0.0	94.6	0.0	5.2

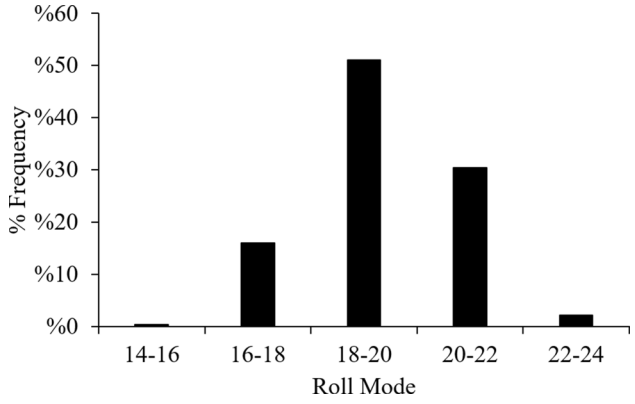

Fig. 6 Histogram of the powertrain roll mode

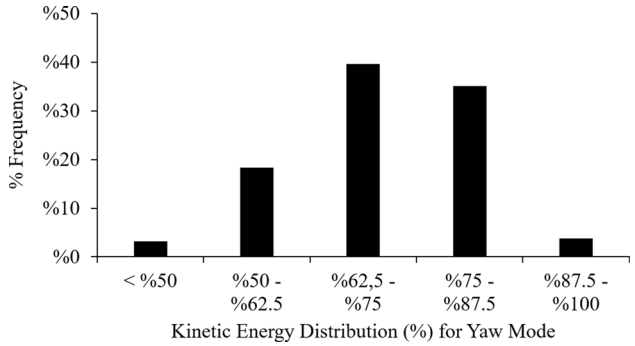

Fig. 7 Histogram of the KED of the powertrain yaw mode

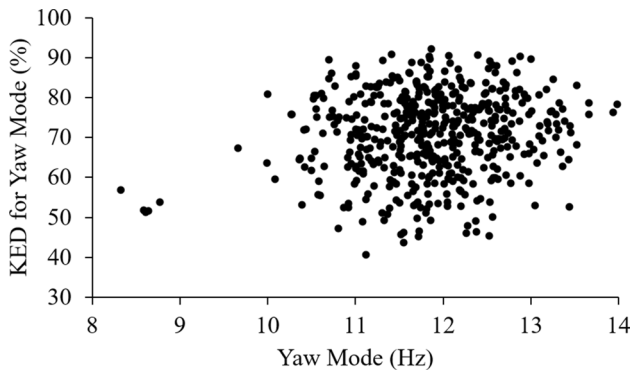

Fig. 8 KED of yaw mode versus yaw mode

mode is presented in Fig. 8. The statistics of the frequency of powertrain modes and their KEDs are summarized in Table 5, and Box-Whisker plot is shown in Fig. 9.

Table 5 Variational results on frequencies of powertrain modes and KEDs

Description	Low	High	Average
Frequency of powertrain lateral mode (Hz)	7.4	11.3	8.6
KED lateral mode (%)	44.0	96.8	76.1
Frequency of powertrain pitch mode (Hz)	6.9	10.6	8.7
KED pitch mode (%)	73.7	99.9	95.1
Frequency of powertrain yaw mode (Hz)	8.3	14.0	11.9
KED yaw mode (%)	40.7	92.2	70.7
Frequency of powertrain vertical mode (Hz)	11.1	13.8	12.5
KED vertical mode (%)	57.8	99.9	95.1
Frequency of powertrain fore-Aft mode (Hz)	16.1	19.8	18.0
KED fore-aft mode (%)	50.7	99.9	96.6
Frequency of powertrain roll mode (Hz)	15.6	23.0	19.4
KED roll mode (%)	48.0	98.4	92.3

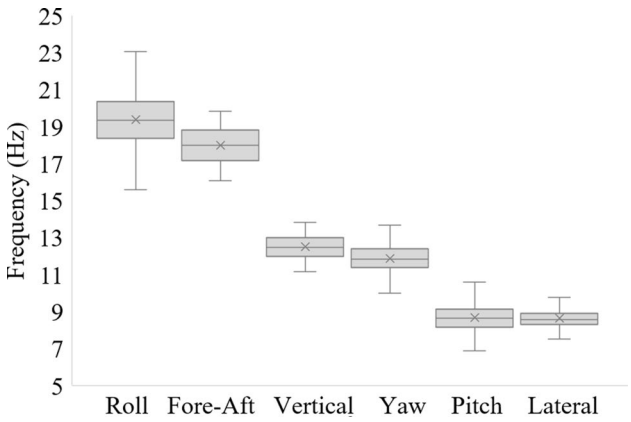

Fig. 9 Box-Whisker plot

3.3 Response surface models

The coefficients of the RSMs from Eq. (2) were calculated using MATLAB's "lsqcurvefit" function as described in Sect. 2.2 and summarized for frequency of powertrain lateral, pitch, yaw, vertical, fore-aft, and roll modes in Table 6. Similarly, the coefficients of the RSMs for KED of each rigid body mode are presented in Table 7.

3.4 Design sensitivity analysis

The design sensitivity analysis is performed to investigate how sensitive the design parameters on the frequencies of powertrain modes and their KEDs. For that purpose, the methods from Sect. 2.4 are applied to quantify the sensitivity of each design parameter on the aforementioned metrics.

PRCC coefficients for the frequencies of powertrain rigid body modes and their KEDs are shown in Tables 8 and 9, respectively.

Table 6 RSM model for the frequency of powertrain rigid body modes

Coefficients	Lateral f_l	Pitch f_p	Yaw f_y	Vertical f_v	Fore-aft f_{fa}	Roll f_r
c_0	0.0836	0.2542	0.2206	−0.0294	0.0684	−0.0862
c_1	−0.0392	−0.3931	−0.0221	0.0189	−0.0035	−0.0073
c_2	0.0341	−0.0006	0.0227	0.0011	−0.0006	0.1453
c_3	0.0028	0.0300	0.0266	0.0011	−0.0077	−0.0295
c_4	−0.2036	0.3308	0.2407	0.1090	0.0040	0.0201
c_5	0.1069	−0.0016	0.2716	0.0025	−0.0005	0.4784
c_6	0.1086	0.0154	−0.1704	0.0048	−0.0901	0.0715
c_7	0.0174	0.0051	0.0091	0.0003	0.0764	0.0051
c_8	0.1015	−0.0004	0.0157	0.0008	0.0006	0.0002
c_9	0.0035	0.3727	0.0158	0.1847	0.0021	0.1101
c_{10}	0.0858	−0.0005	0.1735	0.0020	0.8843	0.0593
c_{11}	0.2264	0.0006	0.1636	−0.0019	0.0004	0.0134
c_{12}	−0.0086	0.0948	0.0524	0.7463	0.0013	0.3234

Table 7 RSM model for KEDs

Coefficients	KED lateral	KED pitch	KED yaw	KED vertical	KED fore-aft	KED roll
c_0	0.3823	0.8955	0.5303	1.0271	0.8273	0.8872
c_1	−0.0778	−0.0001	−0.0752	−0.0263	0.0184	0.0203
c_2	0.0335	−0.0095	0.0730	0.0298	0.0295	0.0549
c_3	0.0540	0.0135	0.0356	−0.0269	0.0319	0.0363
c_4	−0.0308	−0.3309	−0.1027	−0.2113	−0.0480	−0.0806
c_5	0.4052	0.0000	0.3199	−0.0471	0.0813	0.0805
c_6	0.0588	0.1711	−0.0806	−0.0043	0.1217	−0.0928
c_7	0.0261	0.0044	0.0199	0.0051	0.0135	0.0031
c_8	0.0585	0.0027	0.0424	−0.0007	−0.0320	−0.0328
c_9	0.0220	0.1202	0.0510	0.0855	0.0276	0.0577
c_{10}	0.2829	0.0034	0.1812	−0.0122	−0.0580	−0.1244
c_{11}	−0.4238	−0.0062	−0.3987	−0.0330	−0.0231	−0.0417
c_{12}	0.0354	−0.1329	0.1189	−0.0170	0.0420	0.1193

Table 8 PRCC for the frequencies of powertrain rigid body modes

	Lateral mode Mode	Pitch mode	Yaw mode	Vertical mode	Fore-aft	Roll mode
x_{fr}	−0.176	−0.925	−0.115	−0.306	−0.196	−0.070
y_{fr}	0.223	0.058	0.197	−0.040	−0.174	0.756
z_{fr}	0.163	0.164	0.046	0.089	−0.021	−0.204
x_{rr}	−0.312	0.732	0.370	0.475	0.108	0.096
y_{rr}	0.352	0.063	0.530	−0.058	−0.135	0.829
z_{rr}	0.072	−0.036	−0.504	−0.009	−0.699	0.385
K_{fx}	0.202	0.126	0.164	0.060	0.824	−0.261
K_{fy}	0.709	−0.006	0.249	−0.420	0.153	0.000
K_{fz}	0.004	0.865	0.025	0.661	0.081	0.262
K_{rx}	0.261	0.159	0.204	0.063	0.992	−0.250
K_{ry}	0.808	0.017	0.707	−0.041	0.173	0.061
K_{rz}	−0.013	0.455	0.024	0.910	−0.018	0.338

Table 9 PRCC for KEDs

	Lateral	Pitch	Yaw	Vertical	Fore-aft	Roll
x_{fr}	−0.262	−0.020	−0.043	0.005	−0.069	0.127
y_{fr}	0.054	0.012	0.097	−0.010	−0.045	0.282
z_{fr}	0.158	0.138	0.054	−0.117	−0.049	0.204
x_{rr}	0.000	−0.378	−0.164	−0.062	0.168	−0.305
y_{rr}	0.653	0.064	−0.011	−0.071	0.161	0.044
z_{rr}	0.315	0.110	−0.164	−0.050	0.682	−0.672
K_{fx}	0.100	0.025	0.024	−0.022	0.062	−0.112
K_{fy}	0.231	−0.037	−0.054	0.052	0.056	−0.159
K_{fz}	0.006	0.095	0.044	0.105	−0.107	0.292
K_{rx}	0.583	0.033	−0.057	−0.033	0.192	−0.503
K_{ry}	−0.595	−0.083	−0.089	0.065	−0.070	0.011
K_{rz}	−0.065	−0.111	0.179	0.000	−0.145	0.594

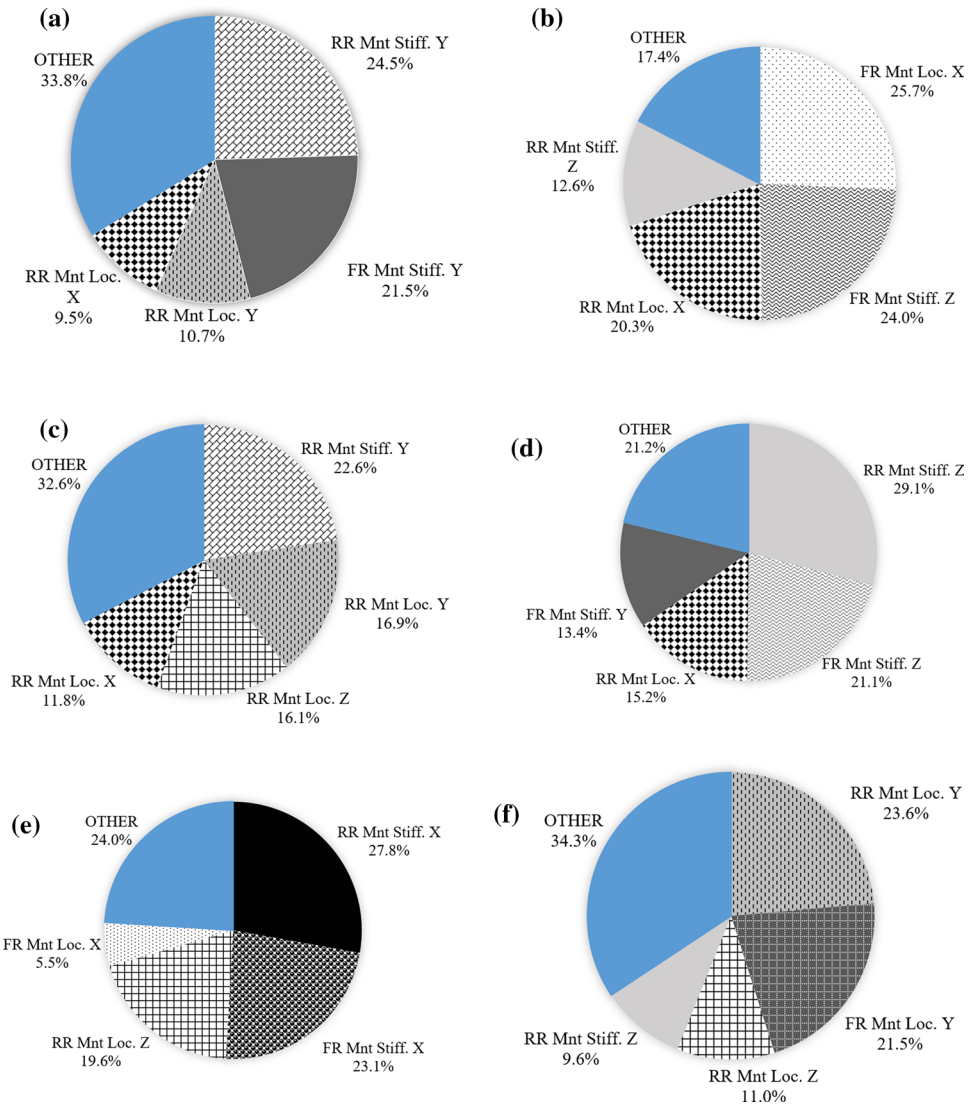

Fig. 10 Sensitivity of modes **a** lateral, **b** pitch, **c** yaw, **d** vertical, **e** fore-aft, **f** roll

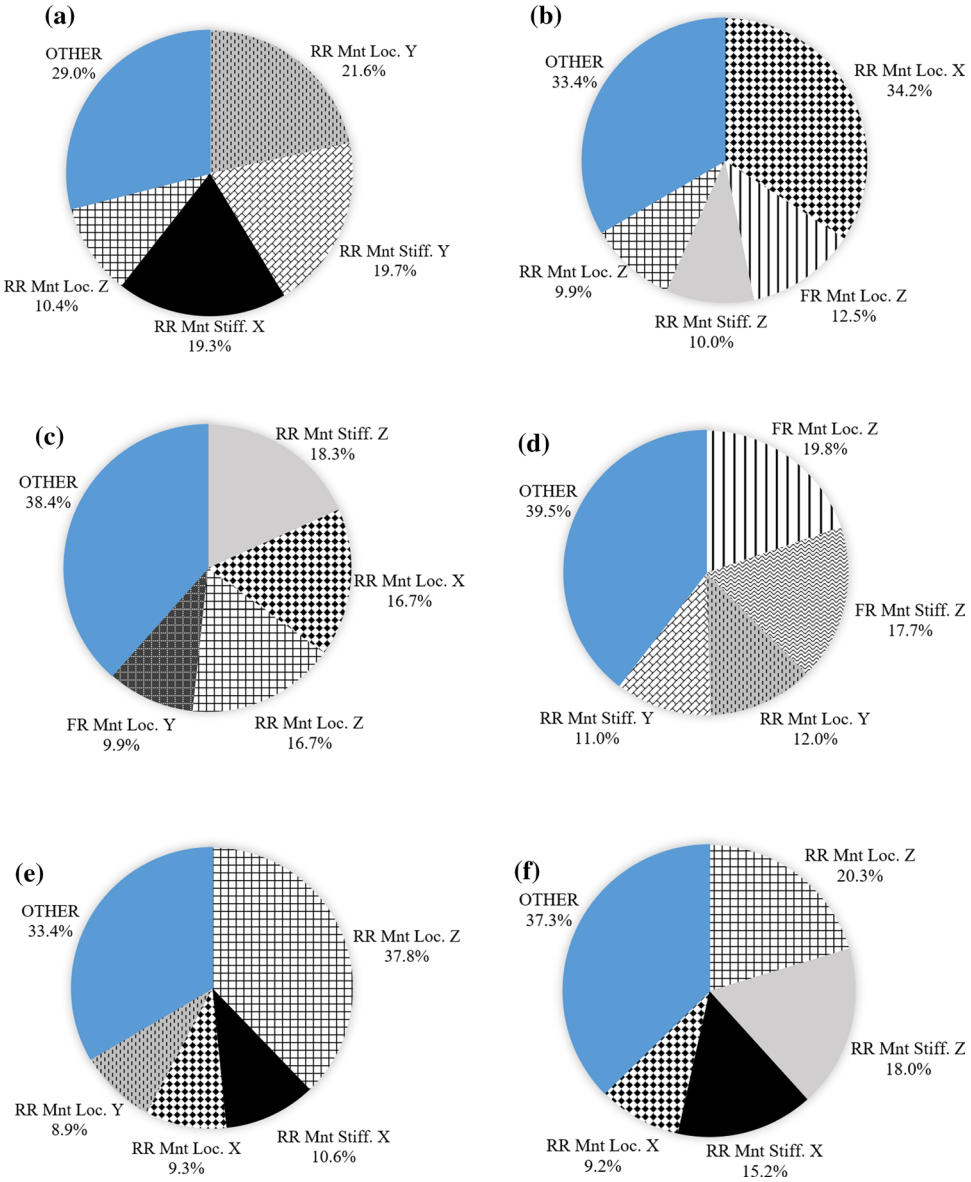

Fig. 11 Sensitivity of KEDs **a** lateral, **b** pitch, **c** yaw, **d** vertical, **e** fore-aft, **f** roll

Frequency of powertrain lateral mode is most sensitive to rear mount stiffness in y-direction (24.5%) and front mount stiffness in the y-direction (21.5%) from Fig. 10a. Rear mount stiffness in the z-direction has little influence on the frequency of powertrain lateral mode, with only 0.1% sensitivity. KED for lateral mode is most sensitive to rear mount location in y-direction (21.6%) and rear mount stiffness in the y-direction (19.7%) from Fig. 11a. Rear mount location in the x-direction and front mount stiffness in the z-direction are not sensitive to KED of the lateral mode with design sensitivities less than 1%.

Front mount location in x-direction and front mount stiffness in the z-direction have the greatest influence on the frequency of powertrain pitch rigid body mode of powertrain with 25.7% and 24%, respectively, as shown in Fig. 10b. It displays very little sensitivity to front and rear mount stiffness in the y-direction and rear mount location in the z-direction all less than 1%. KED for pitch mode is most sensitive to rear mount location in the x-direction (34.2%) and front mount location in the z-direction (12.5%), while it is least sensitive to front mount location in the y-direction (1%) as shown in Fig. 11b.

Rear mount stiffness in the y-direction (22.6%) shows the most influence on the frequency of powertrain yaw mode, followed by rear mount location in the y-direction (16.9%) from Fig. 10c. Both front and rear powertrain mount stiffness in z-direction have minimal influence on yaw mode, less than 1% design sensitivity. Rear mount stiffness in the z-direction (18.3%), rear mount location in the x- and z-directions (16.7% each) have the greatest effect on the KED of the yaw mode, and rear mount location in the y-direction is the least contributing design

parameter to the KED of the yaw mode with 1.1% as shown in Fig. 11c.

Rear mount stiffness in z-direction with 29.1% emerges as the most significant influence on the frequency of powertrain vertical mode of the powertrain followed by front mount stiffness in the z-direction (21.1%) from Fig. 10d. Rear mount location in the z-direction has an influence of only 0.3%. KED of the vertical mode is found to be most sensitive to front mount location in the z-direction (19.8%) and front mount stiffness in the z-direction (17.7%), and least sensitive to rear mount stiffness in the z-direction with less than 1% sensitivity from Fig. 11d.

The frequency of powertrain fore-aft mode is found to be most sensitive to the rear and front powertrain mount stiffness in the x-direction with 27.8% and 23.1%, respectively, as shown in Fig. 10e. Rear mount stiffness in z-direction and front mount location in the z-direction have little influence on the frequency of powertrain lateral mode with less than 1%. Rear mount location in the z-direction (37.8%) and rear mount stiffness in the x-direction (10.6%) have the greatest effect on the KED of the fore-aft mode, and front mount location in the y-direction has the least effect, with only 2.5%, according to Fig. 11e.

Front and rear mount locations in the y-direction have the greatest influence on the frequency of powertrain roll mode, with 21.5% and 23.6%, respectively, as shown in Fig. 10f. It shows very little sensitivity to front mount stiffness in the y-direction with less than 0.1%. KED for roll mode, shown in Fig. 11f, is most sensitive to rear mount location in the z-direction (20.3%) and rear mount stiffness in the z-direction (18%), while it is least sensitive to rear mount stiffness in the y-direction with only 0.3% design sensitivity.

3.5 Design optimization results

The original design (frequencies of the modes and corresponding KEDs are shown in Table 4) does not meet the following design targets:

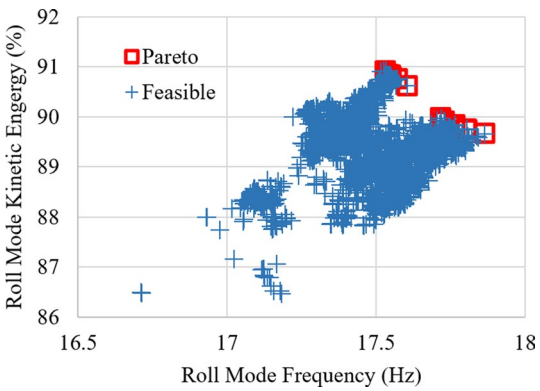

Fig. 12 Feasible and pareto optimal design set

- The frequency of powertrain roll mode of 19.2 Hz is higher than the target frequency of 18 Hz (design target 1).
- The frequency of powertrain vertical mode does not meet the design target 2 since it is not between 8 and 10 Hz.
- The frequencies of powertrain lateral and pitch modes are separated by 0.1 Hz, yaw and lateral modes by 0.5 Hz, fore-aft and roll modes by 1.3 Hz, which are all lower than the target of 1.5 Hz.
- KEDs of lateral (76%) and yaw modes (71.5%) are lower than 80% violating the design target 4.

Variation of rear powertrain mount stiffness in the z-direction, which has the highest contribution of the frequency of powertrain vertical mode, was increased to 2000 mm since the constraint on the frequency of powertrain vertical mode was not satisfied. Feasible design set for which all constraints are met and pareto optimal design set is shown in Fig. 12.

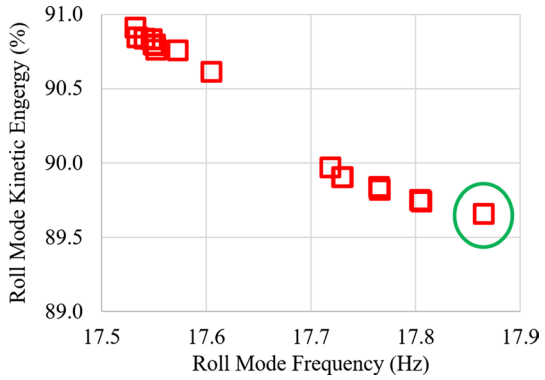

Fig. 13 Pareto frontier and selected optimized design marked by green circle

Table 10 Nominal vs. optimized design

Design Variable	Nominal	Optimized	Change (%)
x_{fr} (mm)	2600	2624	2.2
y_{fr} (mm)	400	447	9.8
z_{fr} (mm)	1250	1288	4.5
x_{rr} (mm)	3800	3733	2.1
y_{rr} (mm)	400	434	9.8
z_{rr} (mm)	1150	1056	8.7
K_{fx} (N/mm)	800	776	2.3
K_{fy} (N/mm)	300	273	6.7
K_{fz} (N/mm)	1200	961	11.1
K_{rx} (N/mm)	9000	10,406	20.0
K_{ry} (N/mm)	2500	2006	20.0
K_{rz} (N/mm)	3500	1988	45.4

Optimum design is selected as the one circled in green in Fig. 13 which has the frequency of powertrain roll mode closer to 18 Hz and highest KED. Other pareto optimal design alternatives are also shown in Fig. 13. Design parameters corresponding to these configurations are shown in Table 10.

The base values of the objective functions, their value after optimization based on RSM models, and the results of ADAMS model using the optimized design variables are shown in Table 11. The frequency of powertrain roll mode from the ADAMS model is 17.7 Hz, which is only 1.6% lower than the target of 18 Hz. KED of the roll mode from ADAMS model is 3.5% lower than the target of 90%. This design target has been met in the optimization study using RSM models. Variation of design constraints is shown in Table 12. The frequency of powertrain vertical mode of 9.9 Hz meets the design target. KEDs of fore-aft, vertical, yaw, pitch, and lateral modes after optimization and also with the ADAMS model are greater than 80%, which met the design targets. The frequencies of the powertrain modes were separated by 1.5 Hz except for pitch and lateral models with ADAMS model. For the later, although the optimization results assured 1.5 Hz separation for those two modes, it is 1.2 Hz with the ADAMS model as a result of the use of response surface models used in the optimization. This can be further improved to meet the design target by increasing the order of polynomials used in the response surface models or by using alternative methods such as genetic algorithms as response surface models.

Table 11 Comparison of design objectives

Metrics	Base	Optimized	RSM (ADAMS)
Frequency of powertrain roll mode (Hz)	19.2	17.9	17.7
KED roll (%)	94.6	89.8	87.3

4 Conclusions

In this study, we investigated the sensitivity of the design parameters of a powertrain mount system on the key performance metrics. For that purpose, a sensitivity and optimization methodology for the determination of powertrain mount locations and stiffness based on the minimization of vehicle level vibration and noise was proposed. The variational design study was explained. The response surface models for the frequency of powertrain rigid body modes and KED's associated with each mode were developed, and an optimization study to place each powertrain rigid body mode at the desired frequency with desired KED was demonstrated on a 4-point powertrain mounting systems. We believe that such a methodology will be beneficial for automotive OEMs to determine the main design parameters at the basic design cycle of an automotive. Besides, such a methodology is expected to resolve conflicting design constraints by the application of a formal optimization algorithm.

These results highlight the importance of a system-level approach to determine the effects of all key design parameters on the frequencies of each powertrain rigid body modes and KEDs associated with them. The complex relationship between the different design factors and the powertrain rigid body modes is especially important as a design guideline in the basic design cycle, where an automotive OEM can see which factor influences the frequencies of powertrain rigid body modes the most and prioritize the development of the design accordingly. The results also suggest that, in designing the powertrain mount systems for improved vibration and noise, it is important to look at the powertrain mount system as a system and not just a single design variable such as mount location or stiffness in the specific axis. Finally, the results of this study also indicate that the different design targets on the frequency of each powertrain mode and its KED make powertrain mount system design quite challenging as shown as a case study in the optimization of the powertrain mount system. The relationship between

Table 12 Comparison of design constraints

Metrics	Base	Optimized	RSM (ADAMS)
Frequency of powertrain fore-aft mode (Hz)	17.9	19.4	19.4
KED fore-aft (%)	99.3	93.8	96.0
Frequency of powertrain vertical mode (Hz)	12.4	10.0	9.9
KED vertical (%)	98.4	97.4	95.9
Frequency of powertrain yaw mode (Hz)	11.9	12.0	12.2
KED yaw (%)	71.5	88.6	81.3
Frequency of powertrain pitch mode (Hz)	8.8	7.0	6.9
KED pitch (%)	98.1	98.1	92.3
Frequency of powertrain lateral mode (Hz)	8.7	8.5	8.1
KED mode (%)	76.0	96.6	90.5

design parameters and proposed metrics was shown to be complex for the simplified model. The inclusion of more design parameters in the sensitivity analysis is likely to add more complexity. Therefore, a formal design sensitivity and optimization in which the coupling effects between various interacting design targets that are explored at every design stage is needed to optimize the powertrain mounting systems. There are also other factors such as the powertrain mass and inertia that were not part of the sensitivity studies, which have an influence on the frequencies of powertrain system modes and their KEDs. These parameters are not varied considering that the automotive manufacturers are more flexible with the design changes related to the powertrain mount location and stiffness. Given the significant role of powertrain mount stiffness on vehicle performance, rubber mount suppliers should focus their attention to manufacture the stiffness properties in different directions and meeting other design targets such as the durability of the mounts.

References

1. Wang X (2010) Vehicle noise and vibration refinement. Woodhead Publishing Limited, Oxford
2. Yu Y, Peelamedu SM, Naganathan NG, Dukkipati RV (2001) Automotive vehicle engine mounting systems: a survey. J Dyn Syst Meas Contr 123:186–194
3. Shangguan W (2009) Engine mounts and powertrain mounting systems: a review. Int J Veh Des 49:237–258
4. Rivin EI (1985) Passive engine mount: some directions for further development. SAE Technical Paper 850481
5. Mita T, Ushijima T (1986) Current review of vibration-insulating rubber products for automobiles. J Soc Autom Eng Jpn 40:1288–1296
6. Yoon JY, Singh R (2011) Estimation of interfacial forces in a multi-degree of freedom isolation system using a dynamic load sensing mount and quasi-linear models. J Sound Vib 330:4429–4446
7. Jung W, Gu Z, Baz A (2010) Mechanical filtering characteristics of passive periodic engine mount. Finite Elem Anal Des 46:685–697
8. Ahn YK, Song JD, Yang BS (2003) Optimal design of engine mount using an artifical life algorithm. J Sound Vib 261:309–328
9. Kim G, Singh R (1995) A study of passive and adaptive hydraulic engine mount systems with emphasis on non-linear characteristics. J Sound Vib 179:427–453
10. Golnaraghi MF, Jazar GN (2001) Development and analysis of a simplified nonlinear model of a hydraulic engine mount. J Vib Control 7:495–526
11. Wang M, Yao GF, Zhao JZ, Qin M (2014) A novel design of semi-active hydraulic mount with wide-band tunable notch frequency. J Sound Vib 333:2196–2211
12. Miller LR, Ahmadian M, Nobles CM, Swanson DA (1995) Modeling and performance of an experimental active vibration isolator. J Vib Acoust 117:272–278
13. Choi WH, Kim JM, Park GJ (2016) Comparison study of some commercial structural optimization software systems. Struct Multidiscip Optim 54(3):685–699
14. Alvarado-Iniesta A, Guillen-Anaya LG, Rodriguez-Picon LA, Neco-Caberta R (2018) Multi-objective optimization of an engine mount design by means of memetic genetic programming and a local exploration approach. J Intell Manuf 1–14
15. Liu CH, Chiang YP, Hsu YY (2018) Optimal design of an elastomeric engine mount with desired stiffness using topology optimization. In: 2018 IEEE/ASME international conference on advanced intelligent mechatronics (AIM), pp 1003–1008
16. Munk DJ, Auld DJ, Steven GP, Vio GA (2019) On the benefits of applying topology optimization to structural design of aircraft components. Struct Multidiscip Optim 60(3):1245–1266
17. Ramesh S, Handal R, Jensen MJ, Rusovici R (2020) Topology optimization and finite element analysis of a jet dragster engine mount. Cogent Eng 7(1):1723821
18. Tao JS, Liu GR, Lam KY (2000) Design optimization of marine engine-mount system. J Sound Vib 235:477–494
19. Ooi L, Ripin ZM (2016) Optimization of an engine mounting system with consideration of frequency dependent stiffness and loss factor. J Vib Control 22:2406–2419
20. Lee DH, Hwang WS, Kim CM (2002) Design sensitivity analysis and optimization of an engine mount system using an FRF-based substructuring method. J Sound Vib 255:383–397
21. Alzahabi B, Mazzei A, Natarajan LK (2003) Investigation of powertrain rigid body modes. In: Conference and exposition on structural dynamics proceedings, 3–6 February 2003, Florida
22. Shangguan WB, Liu XA, Lv ZP, Rakheja S (2016) Design method of automotive powertrain mounting system based on vibration and noise limitations of vehicle level. Mech Syst Signal Process 76–77:677–695
23. Swanson DA, Wu HT, Ashrafiuon H (1993) "Optimization of aircraft engine suspension systems. J Aircr 30:979–984
24. Ashrafiuon H Design optimization of aircraft engine-mount systems. J Vib Acoust 115:463–467
25. Christopherson J, Jazar GN (2005) Optimization of classical hydraulic engine mounts based on RMS method. J Shock Vib 12:119–147
26. Yonghou S, Guocai J (2012) Optimization for powertrain mounting system based on theory of energy decoupling. Adv Mater Res 421:203–207
27. Jeong T, Singh R (2000) Analytical methods of decoupling the automotive engine torque roll axis. J Sound Vib 234:85–114
28. Hafidi E, Martin B, Loredo A et al (2010) Vibration reduction on city buses: determination of optimal position of engine mounts. Mech Syst Signal Process 24:2198–2209
29. Park JY, Singh R (2010) Role of spectrally varying mount properties in influencing coupling between powertrain motions under torque excitation. J Sound Vib 329:2895–2914
30. Hu JF, Singh R (2012) Improved torque roll axis decoupling axiom for a powertrain mounting system in the presence of a compliant base. J Sound Vib 331:1498–1518
31. Liette J, Dreyer JT, Singh R (2014) Critical examination of isolation system design paradigms for a coupled powertrain and frame: partial torque roll axis decoupling methods given practical constraints. J Sound Vib 333:7089–7108
32. Xu X, Su C, Dong P, Liu Y, Wang S (2018) Optimization design of powertrain mounting system considering vibration analysis of multi-excitation. Adv Mech Eng 10(9):1687814018788246
33. Lin J, Lin Z, Ma L, Xu T, Chen D, Zhang J (2019) Analysis and optimization of coupled vibration between substructures of a multi-axle vehicle. J Vib Control 25(5):1031–1043
34. Dao DN, Guo LX (2019) New hybrid between SPEA/R with deep neural network: application to predicting the multi-objective optimization of the stiffness parameter for powertrain mount systems. J Low Freq Noise Vib Active Control 1461348419868322
35. Santhosh S, Velmurugan V, Paramasivam V, Thanikaikarasan S (2020) Experimental investigation and comparative analysis of rubber engine mount vibration and noise characteristics. Mater Today Proc 21:638–642

36. Truong NH, Dao DN (2020) New hybrid between NSGA-III with multi-objective particle swarm optimization to multi-objective robust optimization design for powertrain mount system of electric vehicles. Adv Mech Eng 12(2):1687814020904253
37. Zhou H, Liu H, Gao P, Xiang CL (2018) Optimization design and performance analysis of vehicle powertrain mounting system. Chin J Mech Eng 31(1):31
38. Narayanan G, Rezaei K, Nackenhorst U (2016) Fatigue life estimation of aero engine mount structure using Monte Carlo simulation. Int J Fatigue 83:53–58
39. Cai B, Shangguan WB, Lu H (2019) An efficient analysis and optimization method for the powertrain mounting system with hybrid random and interval uncertainties. Eng Optim 1–20
40. Lim J, Jang YS, Chang HS, Park JC, Lee J (2020) Multi-objective genetic algorithm in reliability-based design optimization with sequential statistical modeling: an application to design of engine mounting. Struct Multidiscip Optim 61(3):1253–1271
41. Bian Y, Gao Z, Hu J, Fan M (2019) A semi-active control method for decreasing longitudinal torsional vibration of vehicle engine system: theory and experiments. J Sound Vib 439:413–433
42. Qin Y, Tang X, Jia T, Duan Z, Zhang J, Li Y, Zheng L (2020) Noise and vibration suppression in hybrid electric vehicles: state of the art and challenges. Renew Sustain Energy Rev 124:109782
43. Wang Q, Wang L, Tan L (2011) Automotive vehicle powertrain mounting system optimum design and simulation analysis. In: IAJC-ASEE conference proceedings, 29–30 April (2011), Boston
44. Nastran MSC (2004) Basic dynamic analysis user's guide. MSC. Software Corporation, USA, pp 37–43
45. Yu Y, Naganathan NG, Dukkipati RV (2001) A literature review of automotive vehicle engine mounting systems. Mech Mach Theory 36:123–142
46. Joe S, Kuo FY (2003) Remark on Algorithm 659: implementing Sobol's Quasirandom Sequence Generator. ACM Trans Math Softw 29:49–57
47. Wu J, Dhingra R, Gambhir M, Remais JV (2013) Sensitivity analysis of infectious disease models: methods, advances and their application. J R Soc Interface 10:20121018
48. Hamby DM (1994) A review of techniques for parameter sensitivity analysis of environmental models. Environ Monit Assess 32:135–154
49. Blower SM, Dowlatabadi H (1994) Sensitivity and uncertainty analysis of complex-models of disease transmission—An HIV model, as an example. Int Stat Rev 62:229–243
50. Marino S, Hogue IB, Ray CJ, Kirschner DE (2008) A methodology for performing global uncertainty and sensitivity analysis in systems biology. J Theor Biol 254–1:178–196
51. Duncan A, Su F, Wolf W (1996) Understanding NVH basics. In: International body engineering conference (IBEC) proceedings, 1–3 October, Detroit, pp 111–116
52. Deb K (2009) Multi-objective optimization using evolutionary algorithms. Wiley, Hoboken